Electronic Supplementary Material (ESI) for Physical Chemistry Chemical Physics.
This journal is © the Owner Societies 2015

Electronic Supplementary Information

Parahydrogen Enhanced NMR Reveals Correlations in Selective Hydrogenation of Triple Bonds over Supported Pt Catalyst

Ronghui Zhou,[1] Wei Cheng,[2] Luke M. Neal,[2,3] Evan W. Zhao,[1] Kaylee Ludden,[1]
Helena E. Hagelin-Weaver[2,*] and Clifford R. Bowers[1,*]

[1]Department of Chemistry, University of Florida, Gainesville, FL USA 32611

[2]Department of Chemical Engineering, University of Florida, Gainesville, FL USA 32611

[3]Present address: Department of Chemical & Biomolecular Engineering, North Carolina State University, Raleigh, NC 27695

Contents

I. Catalyst Characterization

CO Chemisorption Measurements.

The active metal surface area was measured using CO chemisorption on a ChemBET 3000™ (Quantachrome Instruments, Inc.). Before the chemisorption measurements, the fresh Pt/TiO_2 catalyst underwent the following treatment: (1) oxidation in a stream of 5% O_2 in helium at 170 °C for 30 min, (2) outgassing in helium for 15 minutes, (3) reduction in a stream of 5% H_2 in nitrogen at 170 °C for 30 min, (4) outgassing in a helium stream at 170 °C for 15 minutes (to remove the H_2 adsorbed on catalyst surfaces), and cooling from 170 °C to room temperature in a helium stream. The reduction temperatures were chosen based on the temperature programmed reduction (TPR) measurement, which indicated that most of the PtO_x on the oxidized catalyst was reduced at 170 °C. After this treatment, the catalyst was subjected to CO titration, where CO pulses are delivered to the catalyst until no further CO adsorption is observed. A CO uptake of 730 μL/g was measured. A qualitative estimation of the average Pt particle size (Φ_{av}) was obtained from the CO adsorption data and the following equation:

$$\Phi_{av} = \frac{1}{S_{av} V_g} \frac{k C_m V_m}{N_a \rho_m} \qquad \text{* MERGEFORMAT (S1)}$$

In this equation, S_{av} is the average stoichiometry: CO:Pt = 1, k is the particle shape factor (a value of 5 was chosen which assumes a cube shape with one side attached to the support and five sides exposed to the environment), V_m is the molar volume, N_a is Avogadro's number, ρ_m is the metal density, V_g is the volume of gas adsorbed per gram of metal, and C_m is the surface density of metal atoms. A C_m value of 1.25×10^{15} atoms/cm^2 was used for Pt. Using Eq. (S1), the average Pt particle size is estimated to be 1.1 nm with a dispersion of 90%.

Scanning Transmission Electron Microscopy (STEM). Micrographs of the 0.7% Pt/TiO_2 catalyst are shown in Figure 1. The STEM images were collected on a probe aberration corrected JEOL JEM-ARM200cF with a cold-field emission electron gun. The STEM high angle annular dark field (HAADF) image was recorded with the JEOL HAADF detector using the following experimental conditions: probe size 7c, CL aperture 30µm, scan speed 32 µs/pixel, and camera length 8 cm, which corresponds to an probe convergence semi-angle of 11 mrad and collection angles of 76-174.6 mrad. The STEM resolution of the microscope is 0.78 Å. The intensity of atomic columns in STEM HAADF images is proportional to the atomic number Z^n, where n is close to 2, and intensity has a monotonic relationship to sample thickness.[37] Due to the large difference in atomic number, the Pt particles are seen as bright areas against the darker TiO_2 background. A histogram of the Pt particle diameters was constructed by analysis of the STEM images using the ImageJ[39] image analysis software. Single Pt atoms were

not included in the distribution as they may easily migrate to the large particles under reaction conditions. Based on the statistics of 200 particles, the average Pt particle size is found to be 1.1 nm with a standard deviation of 0.2 nm, in excellent agreement with the size estimation obtained by CO chemisorption (above).

II. Spectral Simulation and Fitting

SpinDynamica Simulations. The 6 protons of propene are divided into four chemically inequivalent sets, labeled 1-4, with chemical shifts (in ppm) of 5.85, 5.03, 4.91, 1.72, respectively, and non-negligible J-couplings (in Hz) J_{12}=16.8, J_{13}=10, J_{14}=6.4, J_{23}=2.1. The geminal coupling of the methyl group is taken to be 15 Hz. At 400 MHz, each of the sets of protons is weakly coupled with respect to all the others. The variables are defined in the ALTADENA timing diagram shown in Figure S1. The NMR spectrum is acquired on the continuously flowing gas stream. The volume of gas within the NMR receiver coil at the moment of NMR acquisition contains hydrogenation adducts formed over a distribution of reaction times, $P_r(t)$. As these adducts flow out of the reactor and into the NMR magnet, they are subjected to a time-dependent magnetic field, $B_0(t)$. The actual experimental time dependence, depicted in the middle panel of Figure S1, was obtained by converting the field-distance profile (measured with a Gaussmeter) to a time-profile based on the total flow rate and the inner diameter of the PFA tubing.

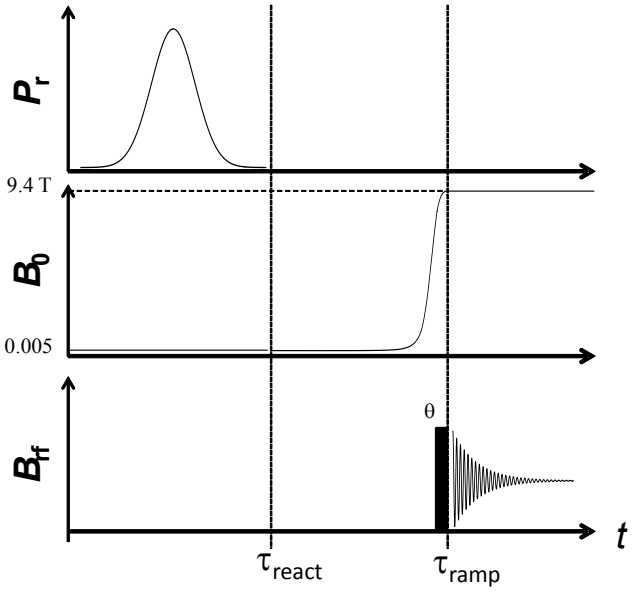

Figure S1. ALTADENA pulse sequence timing diagram illustrating synchronization of NMR pulses (B_{RF}), adiabatic ramping of the static magnetic field (B_0) up to 9.4 T, and distribution of adduct formation times, P_r. The actual magnetic field ramp was obtained by mapping the field profile between the hydrogenation reactor outlet at 5 mT to the magnetic field center of the 9.4 T. The field map was converted to a time-ramp from the diameter of the tubing and the flow rate.

In the Curie-Law regime, the traceless part of the thermal equilibrium density operator for propene can be written

$$\hat{\sigma}_{eq} \propto \sum_{i=1}^{6} \hat{I}_{zi} \qquad \text{* MERGEFORMAT (S2)}$$

ALTADENA spectra are highly dependent on the details of the transport from the (low) reaction field to the (high) detection field. The time dependence of the Zeeman interaction is introduced by incorporating the ramping function $b(t)$ into the rotating frame spin Hamiltonian:

$$\hat{H}_{\text{int}} \propto 2\pi b(t) \sum_i \nu_i \hat{I}_{zi} + 2\pi \sum_{i<j} J_{ij} \hat{\mathbf{I}}_i \cdot \hat{\mathbf{I}}_j \qquad \text{* MERGEFORMAT (S3)}$$

where

$$b(t) = \begin{cases} B_{\text{react}} / B_{\text{detect}} & \text{for } t \le \tau_{\text{react}} \\ B_{\text{ramp}}(t) / B_{\text{detect}} & \text{for } \tau_{\text{react}} < t < \tau_{\text{detect}} \\ 1 & \text{for } t \ge \tau_{\text{detect}} \end{cases} \qquad \text{* MERGEFORMAT (S4)}$$

Here, ν_i is the isotropic chemical shift of the i^{th} spin in the rotating frame. Since the gas is stored in the Earth's field, the 4 protons of the propyne substrate are fully unpolarized. The density operator describing the unpolarized propene proton spin system, excluding the protons originating as p-H_2, is written

$$\hat{\sigma}_{sub} = \hat{1}/16 \qquad \text{* MERGEFORMAT (S5)}$$

The density matrix of H_2 with para- mole fraction χ_p is given by[1]

$$\hat{\sigma}_{para} = \hat{1}/4 - \frac{1}{3}(4\chi_p - 1)\hat{\mathbf{I}}_1 \cdot \hat{\mathbf{I}}_2 \qquad \text{* MERGEFORMAT (S6)}$$

In our propene numbering scheme (sequential in the chemical shift), this density operator would correspond to *anti* addition. For *syn* addition, $\hat{\mathbf{I}}_3$ replaces $\hat{\mathbf{I}}_2$ in Eq. * MERGEFORMAT (S6).

$$\hat{\sigma}^{2,3}_{para} = \hat{1}/4 - \frac{1}{3}(4\chi_p - 1)\hat{\mathbf{I}}_1 \cdot \hat{\mathbf{I}}_{2,3} \qquad \text{* MERGEFORMAT (S7)}$$

The initial density operator

$$\hat{\sigma}^{4}_{para} = \hat{1}/4 - \frac{1}{3}\left(\hat{\mathbf{I}}_1 \cdot \hat{\mathbf{I}}_{4a} + \hat{\mathbf{I}}_1 \cdot \hat{\mathbf{I}}_{4b} + \hat{\mathbf{I}}_1 \cdot \hat{\mathbf{I}}_{4c}\right) \qquad \text{* MERGEFORMAT (S8)}$$

(where *a,b,c* denote each of the methyl protons) models pairwise addition (*syn* or *anti*) followed immediately by double bond migration.

At the instant of adduct formation, the density operator of the product molecule in the expanded basis is given by

$$\hat{\sigma}_{adduct} = \hat{\sigma}_{para} \otimes \hat{\sigma}_{sub} \qquad \text{* MERGEFORMAT (S9)}$$

Following addition, the density operator system evolves under the low field spin Hamiltonian, and the non-secular elements (with respect to the spin Hamiltonian) will oscillate at the Bohr frequencies of the system. Due to variations in the surface residence and transport times in the continuous-flow ALTADENA experiment, the aliquot of molecules within the detected volume of the NMR probe at any instant will contain propene spin systems with varying pairwise addition times. Off-diagonal terms in the density operator wash-out, leaving a time-averaged density operator that is diagonal in the low field Eigenbasis. This is modeled by time-averaging of the density operator:

$$\left\langle \hat{\sigma}_{adduct} \right\rangle = \int_0^{\tau_{react}} P_r(t) e^{i\hat{H}_{\text{int}}t} \hat{\sigma}_{adduct} e^{-i\hat{H}_{\text{int}}t} dt \qquad \text{* MERGEFORMAT (S10)}$$

For a distribution of reaction times that is broad compared to the longest Bohr period in the system, these coherences will vanish. This is efficiently simulated by "secularizing" $\hat{\sigma}_{adduct}$ with respect to $\hat{H}_{\text{int}}$. As adducts flow out of the reactor and into the NMR magnet, they are subjected to a magnetic field ramp, $B_0(t)$. The evolution during the transport to high field is calculated from

$$\hat{\sigma}_0 = U \left\langle \hat{\sigma}_{adduct} \right\rangle U^{\dagger} \qquad \text{* MERGEFORMAT (S11)}$$

where

$$U = \exp\left(-i \int_0^{\tau_{ramp}} d\tau \hat{H}_{\text{int}}(\tau) \right) \qquad \text{* MERGEFORMAT (S12)}$$

Applying the detection pulse with rotation angle θ,

$$\hat{\sigma}_{mix} = e^{i\theta \hat{I}_x} \hat{\sigma}_0 e^{-i\theta \hat{I}_x} \qquad \text{* MERGEFORMAT (S13)}$$

Finally, the frequency spectrum is calculated from

$$S(\nu) = \text{Re}\left\{ \mathcal{F}\left\{ \text{Tr}\{ \hat{I}_+ e^{i\hat{H}_{\text{int}}t} \hat{\sigma}_{mix} e^{-i\hat{H}_{\text{int}}t} \} \right\} \right\} \qquad \text{* MERGEFORMAT (S14)}$$

where $\mathcal{F}$ denotes Fourier transformation. The six spin spectral simulations implementing eqn * MERGEFORMAT (S2)-* MERGEFORMAT (S14) were performed using SpinDynamica v2.8.3 with Wolfram's Mathematica version 8.0.0.0 using an Intel® Core™ I-5 2500K CPU @ 4.2 GHz.

Validation of Simulations and Spectral Fitting Methodology. The density matrix simulations and fitting protocol for determination of syn addition stereoselectivity was validated by two different methods, described here.

Method I: A series of ALTADENA experiments in which the flip angle θ of the NMR read pulse was incremented from 45° to 90° in 15° steps while fixing all other acquisition parameters and reaction conditions. As is known for the AX spin system, the ALTADENA density operator has the form[4]

$$\hat{\sigma} \propto \hat{I}_{zA}\hat{I}_{zB} \pm \frac{1}{2}\left(\hat{I}_{zA} - \hat{I}_{zB}\right)$$ * MERGEFORMAT (S15)

Conversion of the first product operator term in Eq. * MERGEFORMAT (S15) into observable antiphase magnetization is optimized using $\theta = 45^{o}$ and vanishes for 90°. The second term, known as net alignment, is maximized by a 90° pulse. Analogous terms appear in the 6-spin density operator for propene formed by pairwise addition of p-H_2 to propyne. By varying θ, the relative contributions of the two types of spin order to the observed spectrum are varied. As can be seen in Figure S2, substantial changes in the experimental line shapes of the propene CH_2 protons are seen across the series of spectra acquired at $\theta = 45$, 60, 75, and 90° at 350 °C. SpinDynamica spectral simulations for pairwise *syn* and *anti* addition to propyne were performed for the same set of θ used in the collecting of the experimental spectra. For each θ, the experimental spectrum was fit to a linear combination of the simulated *syn* and *anti* addition spectra and the best-fit values of the weighting coefficients were then used to calculate the *syn* addition stereoselectivity. The fits, which are superimposed on the experimental spectra in Figure S2, yield a consistent *syn* addition stereoselectivity of 90 ± 2 % across the series of different flip angles.

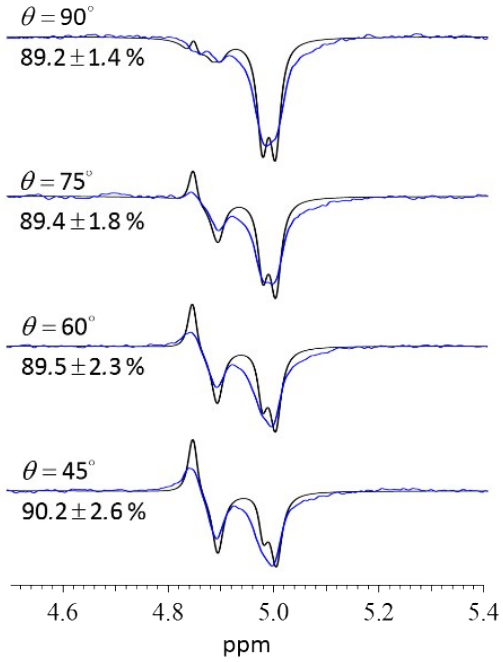

Figure S2. Least-squares fits (black traces) obtained from experimental ALTADENA spectra (in blue) acquired for a 260/120/20 mL/min $N_2/H_2/C_3H_4$ reactant gas mixture (6:1 H_2:propyne, total flow rate of 400 mL/min, 1 bar total pressure) at a reaction temperature of 350 °C for four different NMR pulse flip angles: 45°, 60°, 75° and 90°. Pairwise *syn* addition stereoselectivity, together with confidence intervals from the least squares fitting, are indicated on each spectrum.

Method 2: The hydrogenation reactor bed was moved to a position just a few cm above the NMR probe within the bore of the 9.4 T superconducting NMR magnet. At this reaction field, which was measured to be 2.7 T using a Gaussmeter, the density matrix spectral simulations (Fig. S3) show that there is negligible polarization transfer

to ancillary protons not belonging to one of the magnetically equivalent sets incorporating the protons originating as parahydrogen. Negligible polarization of the propene CH_3 signal is observed, and syn and anti addition yields signal at only the H^3 and H^2 positions, respectively.

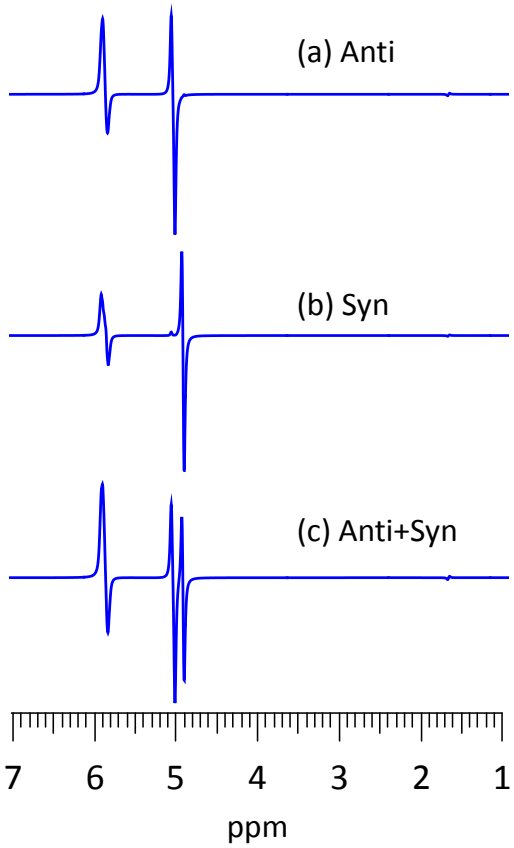

Figure S3. PASADENA SpinDynamica density matrix spectral simulation of propene formed by (a) anti addition, (b) syn addition, or (c) equal amounts of anti and syn addition of parahydrogen to propyne at 2.7 T followed by adiabatic transport to 9.4 T for detection with 45° mixing pulse. A 12 Hz Lorentzian line-broadening was applied.

The PASADENA and ALTADENA mode spectra presented in Fig. S4 were collected using the same Pt/TiO_2 catalyst, reactor, reaction conditions, and acquisition parameters. Stereoselectivity was determined by spectral fitting to linear combinations of the spectra simulated for syn and anti addition using Eq. 1 in the main text. Stereoselectivities determined by fitting the PASADENA and ALTADENA spectra, reported in Fig. S4, are within experimental error the same.

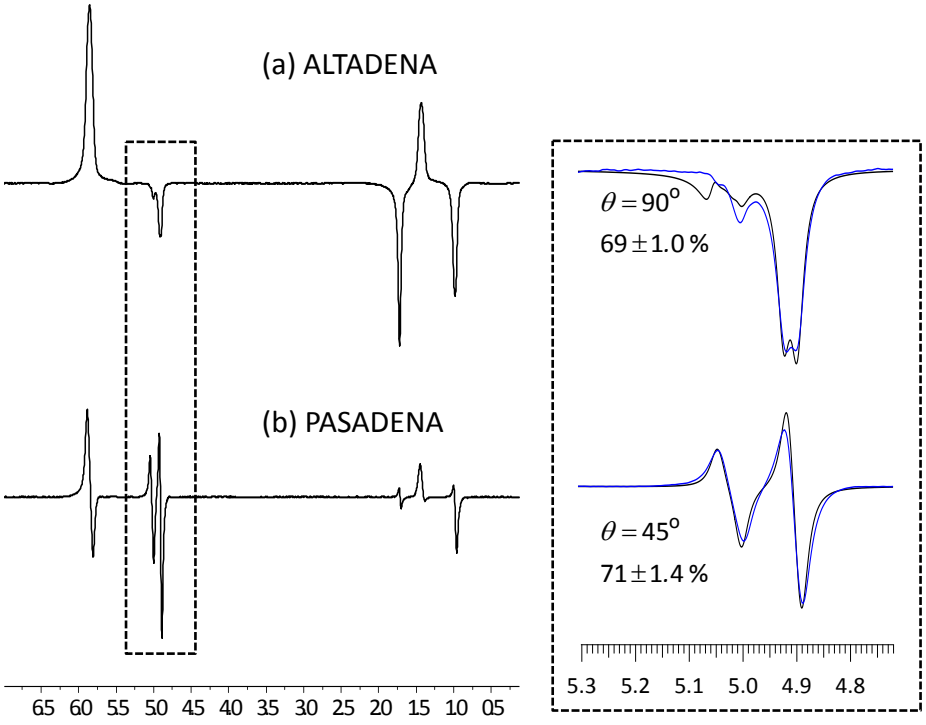

Figure S4. (a) ATLADENA and (b) PASADENA experimental spectra (in blue) acquired for a 160/240/20 mL/min $N_2/H_2/C_3H_4$ reactant gas mixture (6:1 H_2:propyne, total flow rate of 400 mL/min, 1 bar total pressure) at a reaction temperature of 250 °C using an NMR pulse flip angle of 45°. Pairwise *syn* addition stereoselectivity, together with confidence intervals from the least squares fitting, are indicated on each spectrum. The small antiphase CH_3 peak seen in the PASADENA spectrum is attributed to double bond migration.

III. Transport Relaxation Correction

The dependence of the thermally polarized signal on flow rate for pure propene and propane is plotted in Figure S5. This plot is used to estimate relaxation effects during transport of hyperpolarized and unpolarized propene and propane from the reactor outlet at 5 mT to the high magnetic field at 9.4 T.

Flow rate f was converted to transit time using the volume V of the tubing connecting the reactor outlet to the NMR tube:

$$t_{tr} = V / f$$ * MERGEFORMAT (S16)

The relaxation correction factor was obtained by fitting to the following expression to obtain T_{eff}:

$$C_{TP} = 1 - e^{-t_{tr}/T_{eff}}$$ * MERGEFORMAT (S17)

Hence, the signal of the gas fully equilibrated in the field (S^{eq}) could be obtained from the observed gas signal S^{obs}:

$$S_{TP}^{eq} = S_{TP}^{obs} / C_{TP}$$ * MERGEFORMAT (S18)

ALTADENA hyperpolarized signals S^{HP} also suffer from relaxation:

$$S_{HP} = S_{TP}^{obs} / C_{HP}$$ * MERGEFORMAT (S19)

where the correction factor C_{HP} for the polarized signals is

$$C_{HP} = \mathrm{e}^{-t/T_{eff}}$$ * MERGEFORMAT (S20)

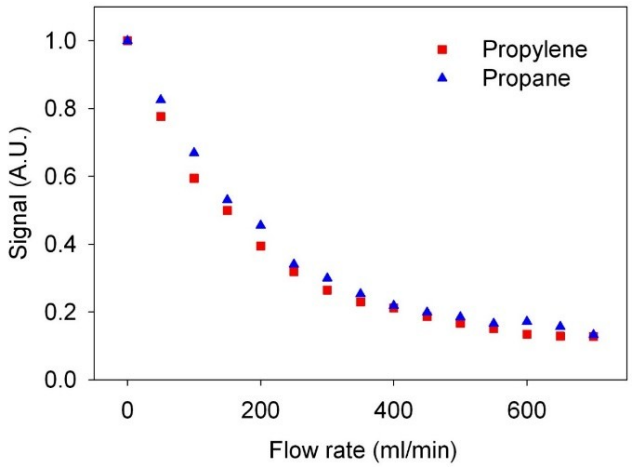

Figure S5. Flow rate dependence of magnetization buildup for propylene and propane (based on the integral values of propylene-CH_3 and propane-CH_2 groups). Integral values were normalized to that of the static spectrum of propylene and propane respectively.

Correction factors for our system are reported in Table S1:

Table S1

	Flow rate	Transport	Propylene			Propane	
	mL/min	t_{tr} (s)	CH	CH_2	CH_3	CH_2	CH_3
T_{eff} (s)	NA	NA	3.22	3.39	2.24	1.94	2.34
	300	0.69	0.19	0.18	0.27	0.30	0.26
	400	0.52	0.15	0.14	0.21	0.23	0.20
C_{TP}	500	0.41	0.12	0.11	0.17	0.19	0.16
	600	0.35	0.10	0.10	0.14	0.16	0.14
	700	0.30	0.09	0.08	0.12	0.14	0.12

IV. Supplemental Spectra

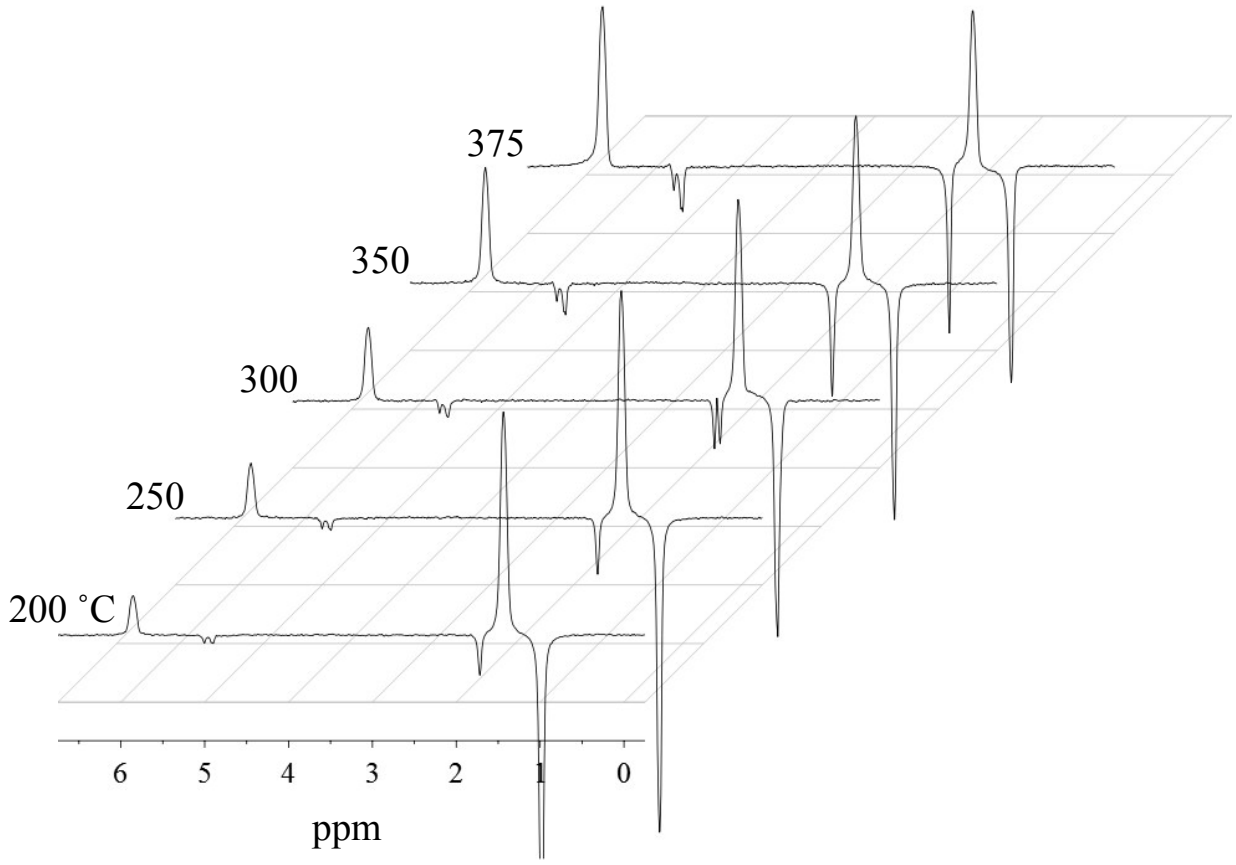

Figure S6. ALTADENA difference spectra collected at a series of temperatures indicated using a fixed 260/120/20 mL/min $N_2/H_2/C_3H_4$ reactant gas mixture (6:1 H_2:propyne) containing p-H_2.

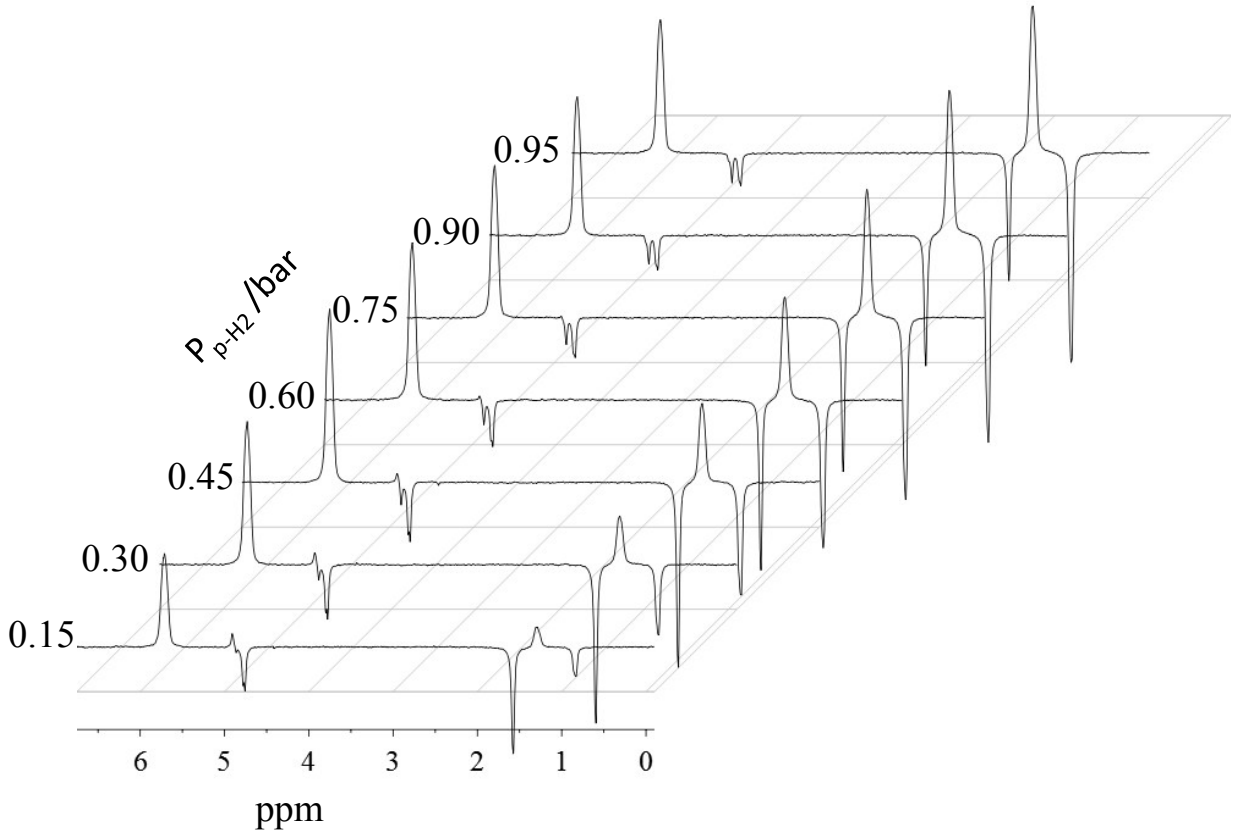

Figure S7. ALTADENA difference spectra (as explained in the main text) recorded at 350 °C using 50 mg catalyst, 0.05 bar propyne, and varying p-H_2 pressure.

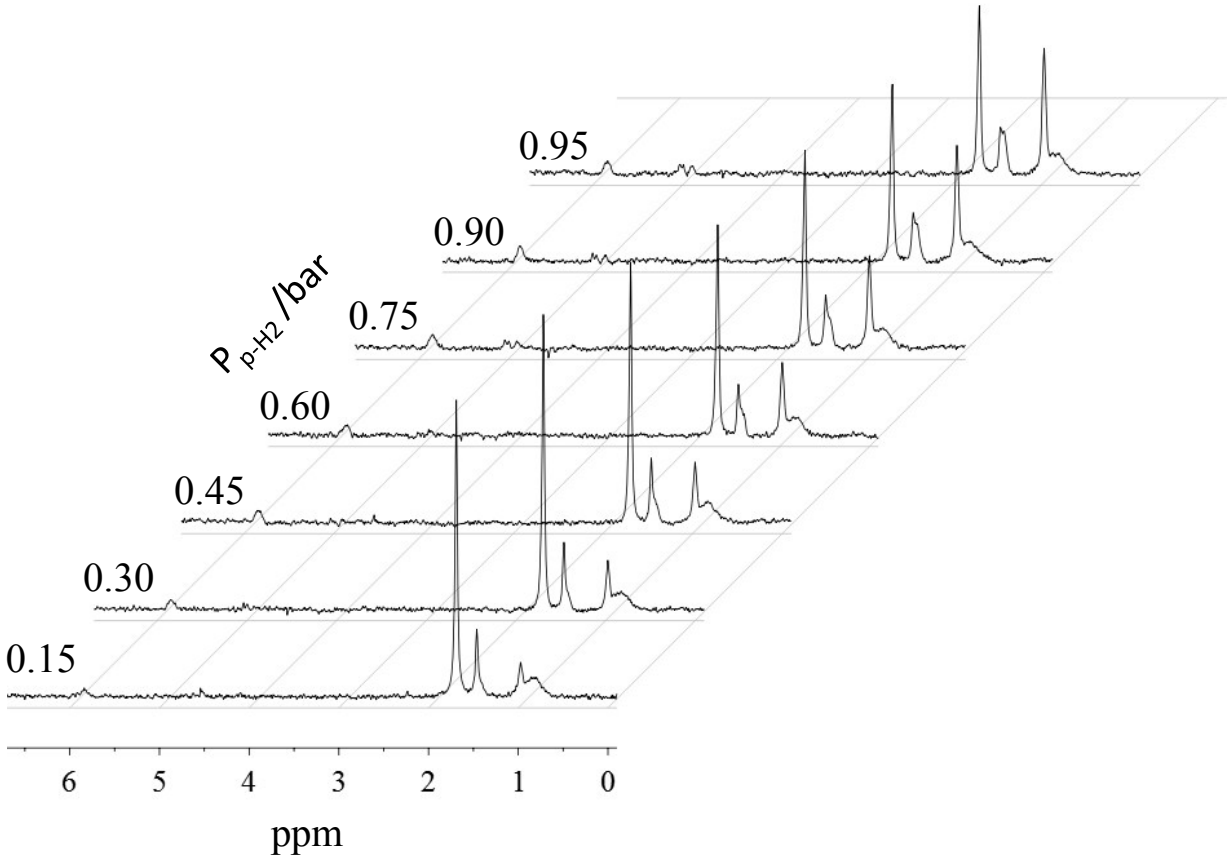

Figure S8. Thermally polarized spectra recorded at 350 °C using 50 mg catalyst, 0.05 bar propyne, varying n-H_2 pressure.

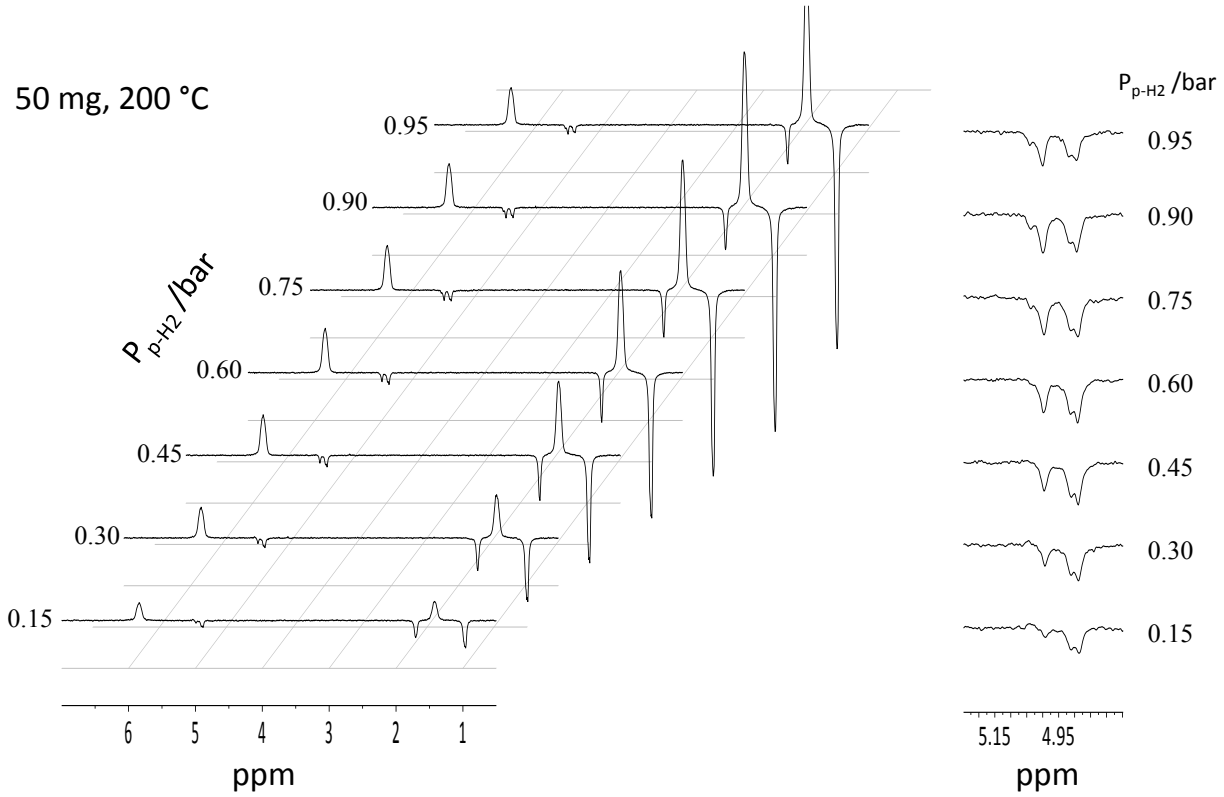

Figure S9. ALTADENA difference recorded at 200 °C, 50 mg catalyst, 0.05 bar propyne and varying p-H_2 pressure.